



Indian Journal of Pure & Applied Physics
Vol. 58, December 2020, pp. 877-884



Time-dependent oscillatory MHD flow over a porous vertical sheet with heat source and chemical reaction effects

Ram Prakash Sharma^{a*}, M C Raju^b, S K Ghosh^c, S R Mishra^d & Seema Tinker^e

^aDepartment of Mechanical Engineering, National Institute of Technology Arunachal Pradesh, Yupia, Papum Pare District, Arunachal Pradesh -791 112, India

^bDepartment of Mathematics, Jawaharlal Nehru Technological University Anantapur, College of Engineering Pulivendula - (Autonomous) Pulivendula 516 390, Arunachal Pradesh India

^cDepartment of Mathematics, Narajole Raj College, Narajole 721 211, West Bengal, India

^dDepartment of Mathematics, S 'O' A Deemed to be University, Khandagiri, Bhubaneswar-751 030, Odisha, India

^eDepartment of Mathematics, JECRC University Jaipur, Rajasthan, 303905, India

Received 29 March 2020; accepted 19 October 2020

The current investigation focuses on unsteady, natural convection viscous incompressible, electrically conducting liquid motion over a vertical plane sheet flooded with permeable media with heat source and chemical reaction. A uniform magnetic field is applied in the transverse direction; the liquid augments in the water way determined by identical pressure, the transport of heat is inclined by radiation. The governing equations are solved by applying the perturbation method. The velocity, heat, and mass profiles are shown on graphs for different physical parameters.

Keywords: MHD oscillatory flow, porous media, Chemical reaction, injection/suction, Heat source

1 Introduction

The transfer of heat from the sheet to the liquid characterizes the appliance of the heat source. The importance of the heat transfer corresponds to the viscous dissipation is vital in several areas such as either in engineering or in industry. Therefore, the appearance dissipation effect on the study of present fluid becomes predominant. The investigations about the under water resources in the field of agriculture engineering as well as see-page of water in the bed of the river *etc.* its application provides a significant contribution. For the filtration and purification process in the chemical engineering, the movement of natural gas in the petroleum engineering and in geothermal reservoir and geothermal energy extractions its application also presents a vital role. Keeping in view, in recent the young scientists have keen interest to develop their thoughts in the said direction. Baag *et al.*¹ investigated the influence of energy source for the transport of heat on the magnetohydrodynamic laminar motion past an extending surface *via* a permeable medium. They

have considered both the assisting and opposing forces to represent the dual behavior of the contributing parameters and then numerical treatment is employed for the transformed governing equations. Mishra *et al.*² have studied the effect of the heat source and thermal radiation on natural convective micropolar liquid motion and transfer of heat past a shrinking surface. Thermal enhancement in the heat transfer phenomenon is observed for the augmentation in the thermal radiation in association with the heat source. Mishra *et al.*³ reported the impact of dissipative heat energy for the combined effects of viscous, Joule and Darcy dissipation on steady laminar boundary layer MHD stagnation-point motion over an extending surface *via* permeable media with heat source /sink. Makinde⁴ studied the effect of the magnetic field and buoyancy forces on heat and mass transfer of an electrically conducting fluid flow over a vertical plate. In the conclusive remarks it is depicted that, the appearance of Lorentz force produces the resistance that resists the fluid motion whereas the both the thermal and solutal buoyancy forces overshoots the profiles as well. Makinde and Ogulu⁵ explored the impact of thermal

*Corresponding author: (E-mail: rpharma@nitap.ac.in)

radiation and magnetic field on the heat and mass transfer of an electrically conducting variable viscosity fluid over a vertical porous sheet. Sharma *et al.*⁶ studied the Soret and diffusion thermoimpact on a 2D non-Newtonian Casson and Williamson fluid motion past a slendering stretching sheet with thermal radiation and variable thickness. Olanrewaju and Makinde⁷ have reported numerically the combined effects of thermal diffusion and diffusion thermo on hydromagnetic boundary layer flow over a permeable sheet. The influence the thermal radiation on the flow of hydromagnetic reacting nanofluid past a heated permeable sheet has been examined by Makinde *et al.*⁸. The diffusion processes conducted for the combined interaction of both energy and solutal profiles presents a significant contributions for the thermal enhancement. Pattnaik *et al.*⁹ have carried out the effect of Dufour and Hall current on unsteady magnetohydrodynamic motion over a perpendicular porous sheet in the presence of suction. The unsteady MHD oscillatory motion of a dusty fluid under the Couette flow scenario in a channel filled with a porous medium under the influence of radiative heat flux and Prakash and Makinde¹⁰ have examined buoyancy force. Ahmed *et al.*¹¹ examined the analytical and numerical solution for MHD three-D motion of Newtonian liquid via a permeable medium past 2-parallel permeable sheets with suction/injection. Jha *et al.*¹² have studied the transient MHD natural convective motion of viscous, incompressible electrically conducting liquid in a vertical permeable passage with thermal radiation and suction/injection. Durga Prasad *et al.*¹³ have explored the transfer of mass and heat study for the unsteady magnetohydrodynamic motion of nanofluid over a rotating an infinite perpendicular porous sheet with chemical reaction and radiation. Misra and Adhikary¹⁴ have analyzed the transfer of mass and heat, magnetohydrodynamic oscillatory motion of blood in a permeable arteriole with chemical reaction. Mahender and Rao¹⁵ have investigated the impact of heat source on unsteady magnetohydrodynamic natural convection and mass shift of motion over a vertical sheet. Bartik *et al.*¹⁶ explored the mixed impact of energy diffusion and heat source on magnetohydrodynamic oscillatory motion *via* a permeable medium over two vertical permeable sheets in the presence of chemical reaction. Noor *et al.*¹⁷ considered the steady magnetohydrodynamic, transfer of energy and mass motion past an inclined surface

with thermophoresis and heat source/sink. Das¹⁸ has analyzed the MHD natural convective transfer of mass and heat motion of a micropolar liquid passing through a permeable media surrounded by an infinite permeable sheet in the presence of heat source. Chen¹⁹ investigated the transfer of heat and MHD flow past an extending surface with an internal heat source/sink.

The purpose of this study is to examine the impacts of the heat source and chemical reaction on unsteady magnetohydrodynamic natural convective energy transport motion of a viscous liquid over a perpendicular sheet. The conservation equations are solved analytically using the perturbation method. Mathematical outcomes are recorded for different values of the objective variables of concern.

2 Mathematical Analysis

The current analysis dispenses with the study of unsteady, free convection viscous incompressible, electrically conducting liquid motion past a vertical channel saturated with permeable media with heat source and chemical reaction effects. A consistent magnetic field has pertained in the oblique direction; the fluid augment in the channel determined by consistent pressure, the heat transport is prejudiced by thermal radiation. The two infinite plates of the vertical channel distanced' apart are porous and the liquid is injected *via* one of the sheets and at the same time sucked through the other with the same velocity. A Cartesian coordinate structure is assumed such that the X^* -axis lies vertically upwards in the direction of the buoyancy force alongside the central line of the channel and Y^* -axis is \perp to the parallel sheets (see Fig. 1). The temperature of the one of the plates is non-uniform and oscillates periodically.

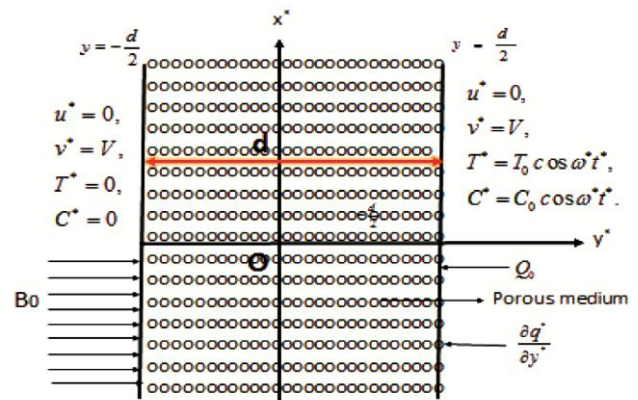


Fig. 1 — Problem geometry

Under the standard Boussinesq approximations, following Magaji²⁰ the motion is governed by the subsequent equations

$$\frac{\partial v^*}{\partial y^*} = 0, \quad \dots (1)$$

$$\frac{\partial u^*}{\partial t^*} + v^* \frac{\partial u^*}{\partial y^*} = -\frac{1}{\rho} \frac{\partial p^*}{\partial x^*} + \nu \frac{\partial^2 u^*}{\partial y^{*2}} - \frac{\sigma B_0^2}{\rho} u^* - \frac{\nu}{K} u^* + g\beta T^* + g\beta_c C^*, \quad \dots (2)$$

$$\frac{\partial T^*}{\partial t^*} + v^* \frac{\partial T^*}{\partial y^*} = \frac{k}{\rho c_p} \frac{\partial^2 T^*}{\partial y^{*2}} - \frac{1}{\rho c_p} \frac{\partial q^*}{\partial y^*} + \frac{Q_0 T^*}{\rho c_p}, \quad \dots (3)$$

$$\frac{\partial C^*}{\partial t^*} + v^* \frac{\partial C^*}{\partial y^*} = D \frac{\partial^2 C^*}{\partial y^{*2}} - k_1 C^*, \quad \dots (4)$$

with

$$y^* = -\frac{d}{2}, u^* = 0, v^* = V, T^* = 0, C^* = 0^*, \quad \dots (5)$$

$$y^* = \frac{d}{2}, u^* = 0, v^* = V, T^* = T_0 \cos \omega^* t^*, C^* = C_0 \cos \omega^* t^*, \quad \dots (6)$$

Subsequently Cogley *et al.*²¹, it is implicit that the liquid is optically thin by comparatively small density. The radiative heat flux is

$$\frac{\partial q^*}{\partial y^*} = 4\alpha^2 T^{* *}, \quad \dots (7)$$

The periodic pressure gradient is

$$-\frac{1}{\rho} \frac{\partial p^*}{\partial x^*} = P \cos \omega^* t^*, \quad \dots (8)$$

Integrating continuity Eq. 1, we get

$$v^* = V. \quad \dots (9)$$

The non-dimensional variables are

$$x = \frac{x^*}{d}, \eta = \frac{y^*}{d}, u = \frac{u^*}{V}, \theta = \frac{T^* - T_0}{T_0}, \phi = \frac{C^* - C_0}{C_0}, t = \omega^* t^*, \omega = \frac{\omega^* d^2}{\nu}, p = \frac{p^*}{\rho V^2}. \quad \dots (10)$$

Substituting Eqs. 9-10 into Eqs. 2-4, we get

$$\omega \frac{\partial u}{\partial t} + \lambda \frac{\partial u}{\partial \eta} = -\lambda \frac{\partial p}{\partial x} + \frac{\partial^2 u}{\partial \eta^2} - M^2 u - \frac{u}{K} + GrT + GmC, \quad \dots (11)$$

$$\omega \frac{\partial \theta}{\partial t} + \lambda \frac{\partial \theta}{\partial \eta} = \frac{1}{Pr} \frac{\partial^2 \theta}{\partial \eta^2} - \frac{1}{Pr} (N^2 - Q)\theta, \quad \dots (12)$$

$$\omega \frac{\partial \phi}{\partial t} + \lambda \frac{\partial \phi}{\partial \eta} = \frac{1}{Sc} \frac{\partial^2 \phi}{\partial \eta^2} - Kr\phi, \quad \dots (13)$$

with

$$u = 0, \theta = 0, \phi = 0, \text{ at } \eta = -\frac{1}{2}, \quad \dots (14)$$

$$u = 0, \theta = \cos t, \phi = \cos t, \text{ at } \eta = \frac{1}{2}, \quad \dots (15)$$

Where,

$$Gr = \frac{g\beta d^2 T_0}{\nu V}, K = \frac{K^*}{d^2}, Pr = \frac{\mu c_p}{k}, N = 2\alpha \frac{d}{\sqrt{k}}, \lambda = \frac{Vd}{\nu}, M = B_0 d \sqrt{\frac{\sigma}{\mu}} \quad \dots (16)$$

$$Gm = \frac{g\beta_c d^2 C_0}{\nu V}, Kr = \frac{d^2 k_1}{\nu}, Sc = \frac{\nu}{D}, Q = \frac{Q_0 d^2}{k}$$

3 Method of Solution

To work out Eq.11-15 for oscillatory motion, following Magaji²⁰ the profiles are assumed as

$$u(\eta, t) = u_0(\eta)e^{it}, \theta(\eta, t) = \theta_0(\eta)e^{it}, \phi(\eta, t) = \phi_0(\eta)e^{it}, -\frac{\partial p}{\partial x} = Pe^{it} \quad \dots (17)$$

Substituting the above expressions into Eqs. 11-15, we obtained

$$u_0'' - \lambda u_0' - (i\omega + K^{-1} + M^2)u_0 = -\lambda P - Gr\theta_0 - Gm\phi_0, \quad \dots (18)$$

$$\theta_0'' - \lambda Pr\theta_0' - (i\omega Pr + N^2 - Q)\theta_0 = 0, \quad \dots (19)$$

$$\phi_0'' - \lambda Sc\phi_0' - (i\omega Sc + krSc)\phi_0 = 0, \quad \dots (20)$$

with

$$u_0 = 0, \theta_0 = 0, \phi_0 = 0 \text{ at } \eta = -\frac{1}{2}, \quad \dots (21)$$

$$u_0 = 0, \theta_0 = 1, \phi_0 = 1 \text{ at } \eta = \frac{1}{2}. \quad \dots (22)$$

Equations 18-22 are solved and the solution for fluid momentum, energy and concentration are given as follows:

$$u(\eta, y) = \left(k_{15} \exp(m_2 \eta) + k_{16} \exp(m_6 \eta) + k_8 - k_9 \exp(m_1 \eta) - k_{10} \exp(m_2 \eta) - k_{11} \exp(m_3 \eta) - k_{12} \exp(m_4 \eta) \right) e^{it}, \quad \dots (23)$$

$$\theta(\eta, y) = (k_2 \exp(m_1 \eta) + k_3 \exp(m_2 \eta)) e^{it}, \quad \dots (24)$$

$$\phi(\eta, y) = (k_5 \exp(m_3 \eta) + k_6 \exp(m_4 \eta)) e^{it}, \quad \dots (25)$$

where the constants are defined as follows:

$$\begin{aligned}
 m_1 &= \frac{\lambda Pr + \sqrt{\lambda^2 Pr^2 + 4k_1}}{2}; m_2 = \frac{\lambda Pr - \sqrt{\lambda^2 Pr^2 + 4k_1}}{2}; k_1 = i\omega Pr + N^2 - Q; k_2 = \frac{e^{(-m_1/2)}}{(e^{m_1} - e^{m_2})}; \\
 k_3 &= -\frac{e^{(-m_1 + m_2/2)}}{(e^{m_1} - e^{m_2})}; \\
 k_4 &= i\omega Sc + KrSc; m_3 = \frac{\lambda Sc + \sqrt{\lambda^2 Sc^2 + 4k_4}}{2}; m_4 = \frac{\lambda Sc - \sqrt{\lambda^2 Sc^2 + 4k_4}}{2}; k_5 = \frac{e^{(-m_1/2)}}{(e^{m_3} - e^{m_4})}; \\
 k_6 &= -\frac{e^{(-m_1 + m_4/2)}}{(e^{m_3} - e^{m_4})}; m_5 = \frac{\lambda + \sqrt{\lambda^2 + 4k_7}}{2}; m_6 = \frac{\lambda - \sqrt{\lambda^2 + 4k_7}}{2}; k_7 = i\omega + K^{-1} + M^2; k_8 = \lambda P / k_7; \\
 k_9 &= \frac{Grk_2}{m_1^2 - \lambda m_1 - k_7}; k_{10} = \frac{Grk_3}{m_2^2 - \lambda m_2 - k_7}; k_{11} = \frac{Gmk_5}{m_3^2 - \lambda m_3 - k_7}; k_{12} = \frac{Gmk_6}{m_4^2 - \lambda m_4 - k_7}; \\
 k_{13} &= k_9 \exp\left(-\frac{m_1}{2}\right) + k_{10} \exp\left(-\frac{m_2}{2}\right) + k_{11} \exp\left(-\frac{m_3}{2}\right) + k_{12} \exp\left(-\frac{m_4}{2}\right) - k_8; \\
 k_{14} &= k_9 \exp\left(\frac{m_1}{2}\right) + k_{10} \exp\left(\frac{m_2}{2}\right) + k_{11} \exp\left(\frac{m_3}{2}\right) + k_{12} \exp\left(\frac{m_4}{2}\right) - k_8; k_{15} = \frac{k_{14} + k_{13} e^{\frac{m_5}{2}}}{(e^{\frac{m_5}{2}} - e^{-\frac{m_5}{2}})}; \\
 k_{15} &= \frac{k_{14} + k_{13} e^{\frac{m_5}{2}}}{(e^{\frac{m_5}{2}} - e^{-\frac{m_5}{2}})}; k_{16} = k_{13} e^{\frac{m_5}{2}} - k_{15} e^{-\frac{m_5}{2}}.
 \end{aligned}$$

The skin-friction τ at the lower sheet is

$$\tau = \left. \frac{\partial u}{\partial \eta} \right|_{\eta=-1/2} = |F| \cos(t + \phi) \quad \dots (26)$$

$$F = F_r + iF_i = (k_{15}m_5 + k_{16}m_6 - k_9m_1 - k_{10}m_2 - k_{11}m_3 - k_{12}m_4) \exp(it), \quad \dots (27)$$

and $|F| = \sqrt{F_r^2 + F_i^2}, \phi = \tan^{-1} \frac{F_i}{F_r} \quad \dots (28)$

The Nusselt-number Nu at the lower sheet is

$$Nu = \left. \frac{\partial \theta}{\partial \eta} \right|_{\eta=-1/2} = |H| \cos(t + \psi) \quad \dots (29)$$

$$H = H_r + iH_i = (k_2m_1 + k_3m_2) \exp(it) \quad \dots (30)$$

and $|H| = \sqrt{H_r^2 + H_i^2}, \psi = \tan^{-1} \frac{H_i}{H_r} \quad \dots (31)$

The Sherwood number Sh at the lower sheet is

$$Nu = \left. \frac{\partial \phi}{\partial \eta} \right|_{\eta=-1/2} = |G| \cos(t + \theta), \quad \dots (32)$$

$$G = G_r + iG_i = (k_5m_3 + k_6m_4) \exp(it), \quad \dots (33)$$

and $|G| = \sqrt{G_r^2 + G_i^2}, \theta = \tan^{-1} \frac{G_i}{G_r} \quad \dots (34)$

4 Results and Discussion

Free convection of a time-dependent flow of a viscous conducting fluid past a heated vertical channel embedding with porous medium is investigated. In addition, the behavior of the heat

source/sink and the first-order chemical reaction is presented in both the energy and solutal transfer equations. To examine the physical perception-into the flow pattern, the mathematical results for the temperature distribution, concentration effects, and velocity distributions are depicted graphically in Figs. 2-9, for dissimilar values of $(Q), (N), (Pr), (\lambda), (Sc), (Kr)$ and (M) . However, Table 1 presents the coincidence of the skin friction and Nusselt number with the results of Magaji²⁰ in the absence of heat source for various values of time parameter. Tables 2, 3 and 4 reveal the mathematical outcomes of the skin friction coefficient, Nusselt number, and Sherwood

Table 1 — Comparative result for the skin friction and Nusselt number at the lower plate for $Q=0$.

| t | τ [20] | τ [Present] | Nu[20] | Nu [Present] |
|-----|-------------|------------------|--------|--------------|
| 0 | 0.6385 | 0.63853142 | 0.9417 | 0.9417127 |
| 0.1 | 1.5105 | 1.51049734 | 0.9249 | 0.9249134 |
| 0.3 | 1.6216 | 1.62163491 | 0.4862 | 0.4862431 |

Table 2 — Variations in skin friction for dissimilar values of momentum parameters

| Gr | Gm | M | K | Pr | Q | N | Sc | Kr | τ |
|----|----|-----|-----|------|-----|-----|------|-----|--------|
| 5 | 5 | 3 | 0.8 | 0.71 | 0.8 | 0.8 | 0.22 | 0.8 | 0.3317 |
| 10 | 5 | 3 | 0.8 | 0.71 | 0.8 | 0.8 | 0.22 | 0.8 | 0.2167 |
| 15 | 5 | 3 | 0.8 | 0.71 | 0.8 | 0.8 | 0.22 | 0.8 | 0.1250 |
| 20 | 5 | 3 | 0.8 | 0.71 | 0.8 | 0.8 | 0.22 | 0.8 | 0.0332 |
| 5 | 10 | 3 | 0.8 | 0.71 | 0.8 | 0.8 | 0.22 | 0.8 | 0.1583 |
| 5 | 15 | 3 | 0.8 | 0.71 | 0.8 | 0.8 | 0.22 | 0.8 | 0.1306 |
| 5 | 20 | 3 | 0.8 | 0.71 | 0.8 | 0.8 | 0.22 | 0.8 | 0.0942 |
| 5 | 5 | 0.5 | 0.8 | 0.71 | 0.8 | 0.8 | 0.22 | 0.8 | 0.0692 |
| 5 | 5 | 1 | 0.8 | 0.71 | 0.8 | 0.8 | 0.22 | 0.8 | 0.1504 |
| 5 | 5 | 2 | 0.8 | 0.71 | 0.8 | 0.8 | 0.22 | 0.8 | 0.1886 |
| 5 | 5 | 3 | 0.1 | 0.71 | 0.8 | 0.8 | 0.22 | 0.8 | 0.0634 |
| 5 | 5 | 3 | 0.3 | 0.71 | 0.8 | 0.8 | 0.22 | 0.8 | 0.0421 |
| 5 | 5 | 3 | 0.5 | 0.71 | 0.8 | 0.8 | 0.22 | 0.8 | 0.0180 |
| 5 | 5 | 3 | 0.8 | 1 | 0.8 | 0.8 | 0.22 | 0.8 | 0.1684 |
| 5 | 5 | 3 | 0.8 | 3 | 0.8 | 0.8 | 0.22 | 0.8 | 0.1838 |
| 5 | 5 | 3 | 0.8 | 7.1 | 0.8 | 0.8 | 0.22 | 0.8 | 0.1972 |
| 5 | 5 | 3 | 0.8 | 0.71 | 0.5 | 0.8 | 0.22 | 0.8 | 0.2472 |
| 5 | 5 | 3 | 0.8 | 0.71 | 1 | 0.8 | 0.22 | 0.8 | 0.2990 |
| 5 | 5 | 3 | 0.8 | 0.71 | 2 | 0.8 | 0.22 | 0.8 | 0.3554 |
| 5 | 5 | 3 | 0.8 | 0.71 | 0.8 | 0.1 | 0.22 | 0.8 | 0.1608 |
| 5 | 5 | 3 | 0.8 | 0.71 | 0.8 | 0.5 | 0.22 | 0.8 | 0.1786 |
| 5 | 5 | 3 | 0.8 | 0.71 | 0.8 | 1 | 0.22 | 0.8 | 0.1820 |
| 5 | 5 | 3 | 0.8 | 0.71 | 0.8 | 0.8 | 0.60 | 0.8 | 0.2575 |
| 5 | 5 | 3 | 0.8 | 0.71 | 0.8 | 0.8 | 0.78 | 0.8 | 0.2798 |
| 5 | 5 | 3 | 0.8 | 0.71 | 0.8 | 0.8 | 0.96 | 0.8 | 0.2883 |
| 5 | 5 | 3 | 0.8 | 0.71 | 0.8 | 0.8 | 0.22 | 1 | 0.4468 |
| 5 | 5 | 3 | 0.8 | 0.71 | 0.8 | 0.8 | 0.22 | 2 | 0.4486 |
| 5 | 5 | 3 | 0.8 | 0.71 | 0.8 | 0.8 | 0.22 | 3 | 0.4498 |

number for different values of evolving parameters. It is interesting to note in Table 2 that an increase in parameter values of M , Pr , Q , N , Sc , and Kr boost the skin friction while the trend is opposite by an enhance in the parameter values of Gr , Gm and K . Meanwhile, the Nusselt number rises by the enhanced values of Pr , Q , and N as exposed in Table 3. In Table 4, it is seen that the Sherwood number escalates with increasing values of Sc and Kr .

Figure 2 depicts the significant behavior of the heat generation/aborption parameter on the fluid temperature. The numerical result indicates the impact

Table 3 — Variations in Nusselt number

| Pr | Q | N | Nu |
|------|-----|-----|--------|
| 0.71 | 0.8 | 0.8 | 1.4626 |
| 1 | 0.8 | 0.8 | 2.3128 |
| 3 | 0.8 | 0.8 | 3.6469 |
| 7.1 | 0.8 | 0.8 | 5.1283 |
| 0.71 | 0.1 | 0.8 | 5.0056 |
| 0.71 | 0.3 | 0.8 | 5.0291 |
| 0.71 | 0.5 | 0.8 | 5.1256 |
| 0.71 | 0.8 | 0.8 | 5.1283 |
| 0.71 | 0.8 | 0.5 | 5.4492 |
| 0.71 | 0.8 | 1 | 5.6524 |
| 0.71 | 0.8 | 2 | 5.8672 |

Table 4 — Variations in Sherwood number

| Sc | Kr | Sh |
|------|-----|--------|
| 0.22 | 0.8 | 3.5484 |
| 0.60 | 0.8 | 4.6542 |
| 0.78 | 0.8 | 4.8492 |
| 0.96 | 0.8 | 5.5321 |
| 0.22 | 0.1 | 3.5234 |
| 0.22 | 0.3 | 3.6134 |
| 0.22 | 0.5 | 3.7568 |
| 0.22 | 0.9 | 3.8829 |

of enhancing values of (Q) results in reducing energy while for negative energy absorption parameter ($-Q$) leads to an increase in the temperature. Figure 3 illustrates the influence of the radiation-conduction parameter (N) on the temperature profiles for $Pr = 0.71$ ($Pr < 1$), so that heat diffuses faster than momentum in the region. With an increase in N *i.e.*, stronger thermal radiation flux, there arise decreasing natures on the temperature profile. A thin case is generally happening with decisive importance to a radiation absorption parameter for an optically thin medium. The significant contribution of the Prandtl number on the fluid temperature is displayed in Fig. 4. It is seen that the enhance in (Pr) the energy description reduces with different values of (Pr). The effect of the Prandtl number plays a significant role in the diffusion concept of flow medium. If Prandtl number

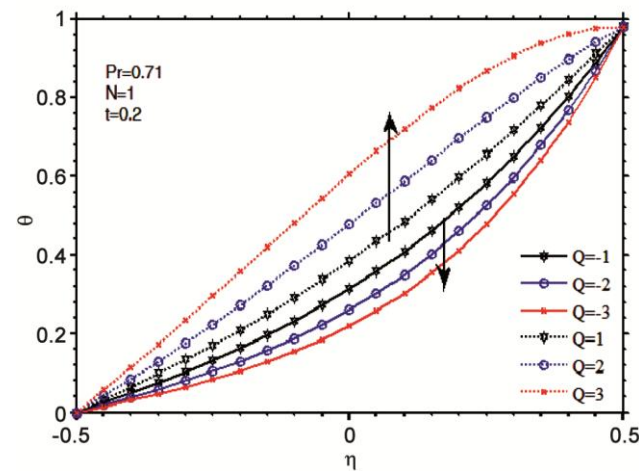


Fig. 2 — Effect of Q on temperature

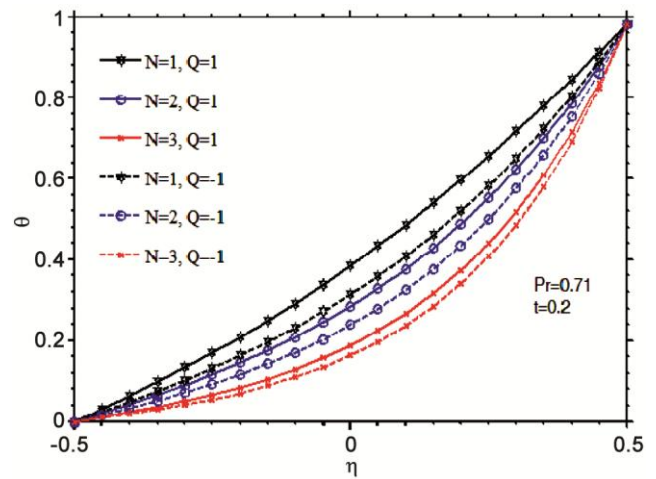


Fig. 3 — Effect of N on temperature

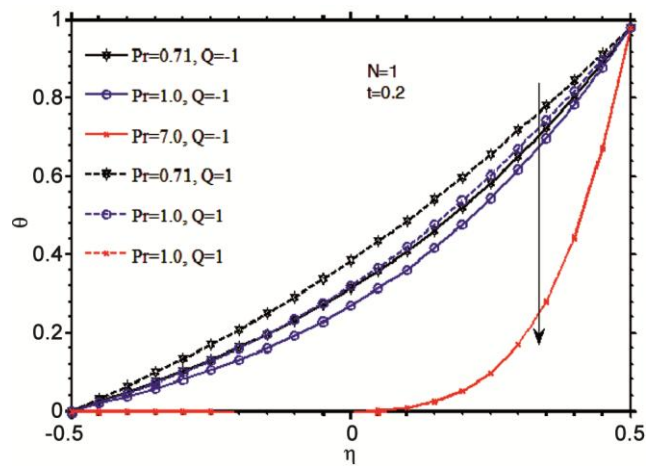


Fig. 4 — Effect of Pr on temperature

is greater than one ($Pr > 1$), the diffusivity of the medium inclines to ionization of the motion. In a high-ionized fluid ($Pr > 1$), the effect of the Prandtl number ($Pr = 7.0$) is transformed from ionized state to water. Figure 5 demonstrates that the energy field enhances with enhance in (λ). In general, the suction parameter is influenced by the heat absorption coefficient (Q) to reduce the temperature field. In a highly permeable medium, the suction parameter is a great deal of advantages to reduce the temperature on the porous medium flow. Figure 6 reveals that the impact of (Sc) on concentration lies in its behavior of a homogeneous reaction concerning a chemical reaction. As Schmidt number increases, it reveals to decrease concentration. The heavier species formed

due to the relationship of the kinematic viscosity and the solutal diffusivity and it is seen that the boost in heavier species suggests that the solutal diffusion retrads that resulted in the concentration profile retrads. Figure 7 depicts the impact of (Kr) on concentration plays a significant role on the behavior of concentration in the flow medium and confirms the observations that an enhance in (Kr) leads to a decrease in concentration. The chemical reaction inhomogeneous systems are characterized by a non-catalytic system where nuclear reaction does not involve in this process. In a permeable medium flow, concentration decreases in a highly permeable medium when the chemical reaction parameter is increased. Therefore, in a permeable medium flow, the effect of chemical reaction leads to decay in

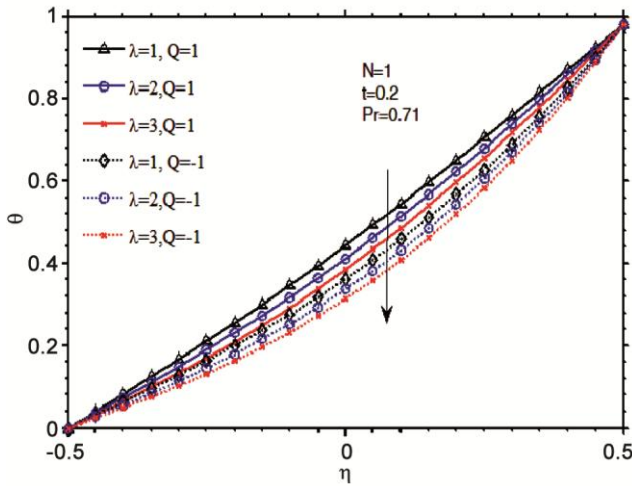


Fig. 5 — Influence of λ on temperature

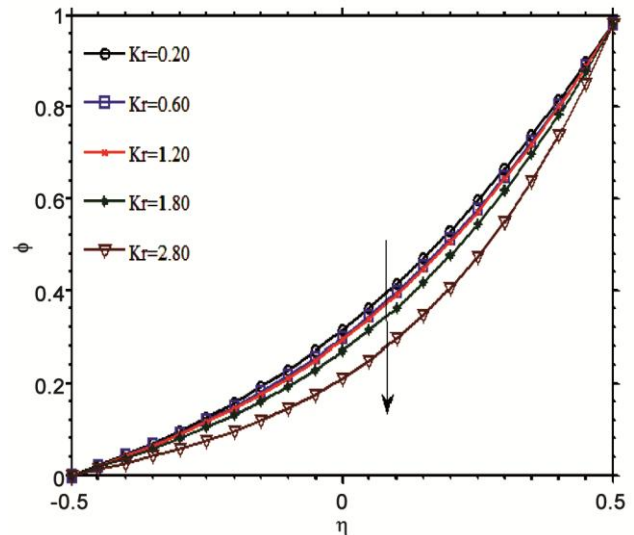


Fig. 7 — Influence of Kr on Concentration

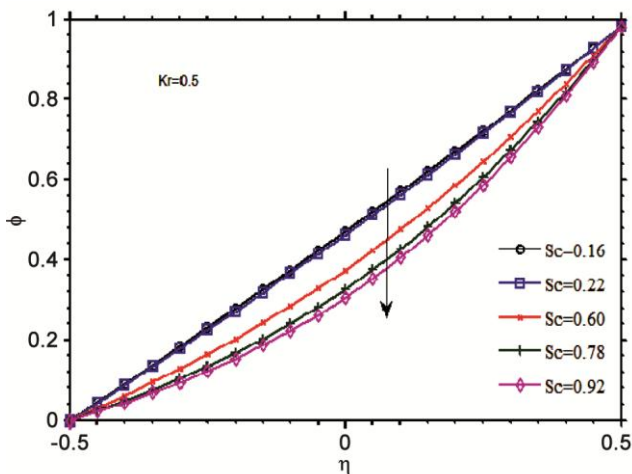


Fig. 6 — Influence of Sc on concentration

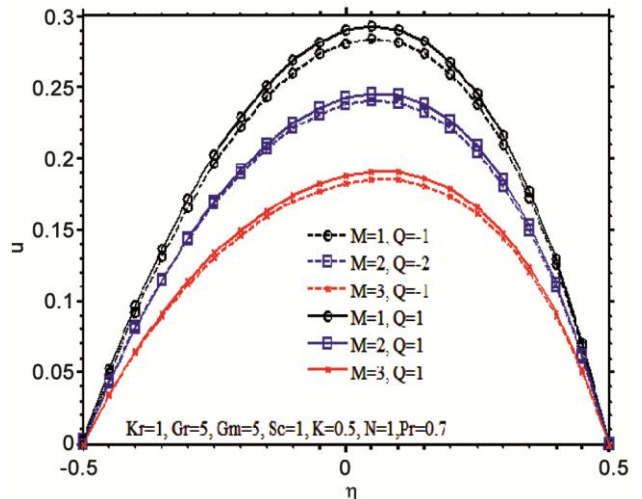


Fig. 8 — Effect of M velocity profile

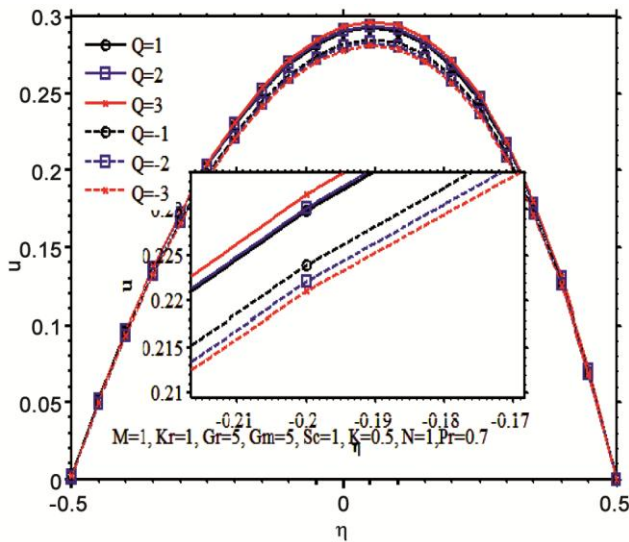


Fig. 9 — Effect of Q on velocity profile

concentration distribution. In Fig. 8 we have presented the impact of Hartmann number (M) on the momentum distribution. With increasing magnetic field strength, M is increases and this serves to decelerate the flow, which leads to reduce momentum because of the occurrence of Lorentz force. The deformation of a magnetic line force experiences a decreasing nature of the velocity field with an increase in magnetic force. Figure 9 shows that the positive value of (Q) the velocity increases with an increase in Q . From another point of view, the velocity reduces with enhance in negative value of (Q). Therefore, the numerical outcomes show that the impact of enhancing values of (Q) outcome an increasing velocity.

5 Conclusions

A mathematical analysis has been presented with transient magnetohydrodynamic combined convective oscillatory motion via a permeable medium subject to a chemical reaction, heat-source and injection/suction enclosed with two vertical permeable sheets. Since the MHD motion is determined by an oscillatory pressure gradient, it is rigorously stated that the flow is oscillatory and simultaneously the heat of one of the sheets is non-uniform and oscillates periodically. The problem is solved analytically by using the perturbation method. An illustration for physical discussions is obtained from the graphical representations on temperature field, concentration and velocity distributions.

References

- Baag S, Mishra S R, Hoque M M & Anika N N, *J Nanofluids*, 7 (2018) 1.
- Mishra S R, Khan I, Al-Mdallal Q M & Asifad T, *Case Studies Thermal Eng*, 11 (2018) 113.
- Mishra S R, Nayak B & Sharma R P, *Defect Diffusion Forum*, 374 (2017) 92.
- Makinde O D, *Int J Num Meth Heat Fluid Flow*, 19 (2009) 546.
- Makinde O D & Ogulu A, *Chem Eng Commun*, 195 (2008) 1575.
- Sharma R P, Avinash K, Sandeep N & Makinde O D, *Defect Diffusion Forum*, 377 (2017) 242.
- Olanrewaju P O & Makinde O D, *Arab J Sci Eng*, 36 (2011) 1607.
- Makinde O D, Das S & Jana R N, *J Nanofluids*, 5 (2016) 687.
- Pattnaik J R, Dash G C & Singh S, *Alexandria Eng J*, 56 (2017) 13.
- Prakash O & Makinde O D, *Latin Am Appl Res*, 45 (2015) 185.
- Ahmed S, Zueco J & López-González L M, *Int J Heat Mass Trans*, 108 (2017) 322.
- Jha B K, Isah B Y & Uwanta I J, *Ain Shams Eng J*, 9 (2016) 1069.
- Prasad P D, Kumar R V M S S K & Varma S V K, *Ain Shams Eng J*, 9 (2018) 801.
- Misra J C & Adhikary S D, *Alexandria Eng J*, 55 (2016) 287.
- Mahender D & Srikanth R P, *J Phys Conf Ser*, 662 (2015) 1.
- Barik R N, *et al.*, *J Appl Anal Comput*, 3 (2013) 307.
- Noor N F, *et al.*, *Int J Heat Mass Trans*, 55 (2012) 2122.
- Das K, *Int J Heat Mass Trans*, 54 (2011) 3505.
- Chen C H, *Int J Heat Mass Trans*, 53 (2010) 4264.
- Magaji A, *J Sci Eng Res*, 3 (2016) 590.
- Cogley C L, Vincenti W G & Gilles E S, *Am Inst Aeron Astron*, 6 (1968) 551.

Nomenclature

| | |
|---------|---|
| g | acceleration due to gravity |
| t | dimensionless time |
| B_0 | transverse magnetic field strength |
| T^* | temperature |
| Sc | Schmidt number |
| T | dimensionless temperature |
| Gr | Grashofnumber due to temperature |
| T_0 | temperature of the plate |
| C_p | specific heat at constant pressure |
| u^* | x -component of velocity |
| D | mass diffusivity |
| u | velocity of the plate |
| k_1^* | chemical reaction parameter |
| V | suction/injection velocity |
| Kr | dimensionless chemical reaction parameter |
| v^* | y -component of velocity |

| | | | |
|----------------------|--------------------------------------|-----------|-----------------------------------|
| κ | thermal conductivity of the fluid | β | volumetric coefficient of thermal |
| ω^* | frequency of oscillations | q^* | radiative heat flux expansion |
| Greek symbols | | | |
| K^* | permeability parameter | N | radiation parameter |
| K | dimensionless permeability parameter | σ | electrical conductivity of fluid |
| α | mean radiation absorption | P | pressure gradient |
| M | magnetic field parameter coefficient | ρ | fluid density |
| Gm | Grashofnumber due to concentration | Q | heat source parameter |
| β_c | volumetric coefficient of | ν | kinematic viscosity |
| Pr | Prandtl number concentration | t^* | time |
| p^* | pressure | λ | suction parameter |